# Integrated Transcriptomic and Epigenomic Analysis of Ovarian Cancer Reveals Epigenetically Silenced *GULP1*

Leonel Maldonado[1, 2#], Mariana Brait[1#], Evgeny Izumchenko[1], Shahnaz Begum[3], Aditi Chatterjee[1,4], Tanusree Sen[1], Myriam Loyo[1,5], Alvaro Barbosa[6], Maria Luana Poeta[7], Eugene Makarev[8], Alex Zhavoronkov[8], Vito M. Fazio[9, 10], Roberto Angioli [11], Carla Rabitti [12], Mate Ongenaert [13], Wim Van Criekinge [13], Maartje G. Noordhuis[1, 14], Pauline de Graeff [14], G. Bea A. Wisman[14], Ate G. J. van der Zee[14], Mohammad O. Hoque[1, 15, 16*].

## ABSTRACT

Many epigenetically inactivated genes involved in ovarian cancer (OC) development and progression remain to be identified. Therefore, in this study we undertook an integrated approach that consisted of identification of genome-wide expression patterns of primary OC samples and normal ovarian surface epithelium along with pharmacologic unmasking strategy using 3 OC and 3 immortalized normal ovarian epithelial cell lines. Our filtering scheme identified 43 OC specific methylated genes and among the 5 top candidates (*GULP1, CLIP4, BAMBI, NT5E, TGFB2*), we performed extended studies of *GULP1*. In a training set, we identified *GULP1* methylation in 21/61(34%) of cases with 100% specificity. In an independent cohort, the observed methylation was 40% (146/365) in OC, 12.5% (2/16) in borderline tumors, 11% (2/18) in cystadenoma and 0% (0/13) in normal ovarian epithelium samples. *GULP1* methylation was associated with clinicopathological parameters such as stage III/IV (p=0.001), poorly differentiated grade (p=0.033), residual disease (p<0.0003), worse overall (p=0.02) and disease specific survival (p=0.01). Depletion of GULP1 in OC cells led to increased pro-survival signaling, inducing survival and colony formation, whereas reconstitution of GULP1 negated these effects, suggesting that GULP1 is required for maintaining cellular growth control.

# Integrated Transcriptomic and Epigenomic Analysis of Ovarian Cancer Reveals Epigenetically Silenced *GULP1*

Leonel Maldonado[1, 2#], Mariana Brait[1#], Evgeny Izumchenko[1], Shahnaz Begum[3], Aditi Chatterjee[1,4], Tanusree Sen[1], Myriam Loyo[1,5], Alvaro Barbosa[6], Maria Luana Poeta[7], Eugene Makarev[8], Alex Zhavoronkov[8], Vito M. Fazio[9, 10], Roberto Angioli [11], Carla Rabitti [12], Mate Ongenaert [13], Wim Van Criekinge [13], Maartje G. Noordhuis[1, 14], Pauline de Graeff [14], G. Bea A. Wisman[14], Ate G. J. van der Zee[14], Mohammad O. Hoque[1, 15, 16*].

[1]Department of Otolaryngology and Head & Neck Surgery, Johns Hopkins University School of Medicine, Baltimore, MD, USA.
[2]Department of Pathology, University of South Alabama Medical Center, Mobile, AL, USA.
[3] Department of Pathology, Johns Hopkins Medical Institutions, Baltimore, MD, USA.
[4]Institute of Bioinformatics, International Technology Park, Bangalore 560 066, India
[5] Department of Otolaryngology-Head and Neck Surgery, Oregon Health and Science University, Portland, OR, USA.
[6] Department of Pathology, Hospital San Jose Tec de Monterrey, Monterrey, Nuevo Leon, Mexico.
[7] Department of Biosciences, Biotechnologies and Biopharmaceutics, University of Bari, Bari, Italy.
[8] Insilico Medicine, Inc, ETC, Johns Hopkins University, Baltimore, MD, USA.
[9] Laboratory of Genetic and Clinical Pathology, University Campus Bio-Medico of Rome, Rome, Italy.
[10] Laboratory of Oncology, IRCCS Casa Sollievo della Sofferenza, San Giovanni Rotondo (FG), Italy.
[11] Department of Gynecology, University Campus Bio-Medico of Rome, Rome, Italy.
[12] Department of Pathology, University Campus Bio-Medico of Rome, Rome, Italy.
[13] Department of Mathematical Modeling, Statistics and Bio-Informatics, Ghent University, Ghent, Belgium.
[14] Department of Gynecologic Oncology, University Medical Center Groningen, University of Groningen, Groningen, The Netherlands.
[15]Department of Oncology, Johns Hopkins University School of Medicine, Baltimore, Maryland, USA.
[16]Department of Urology, Johns Hopkins University School of Medicine, Baltimore, Maryland, USA.

[#] These authors contributed equally to this study (LM and MB)

Running Title: Discovery of the role of *GULP1* in Ovarian Cancer

All named authors have agreed to the submission and have participated in the study to a sufficient extent to be named as authors. The authors declare no potential conflicts of interest.

*Corresponding author:
Mohammad Obaidul Hoque, DDS, Ph.D.
Department of Otolaryngology and Head & Neck Surgery
Johns Hopkins University School of Medicine
1550 Orleans Street, CRB II, 5M06
Baltimore, MD 21231
Phone 410-502-8778
Fax 410-614-1411
mhoque1@jhmi.edu

**ABSTRACT**

Many epigenetically inactivated genes involved in ovarian cancer (OC) development and progression remain to be identified. Therefore, in this study we undertook an integrated approach that consisted of identification of genome-wide expression patterns of primary OC samples and normal ovarian surface epithelium along with pharmacologic unmasking strategy using 3 OC and 3 immortalized normal ovarian epithelial cell lines. Our filtering scheme identified 43 OC specific methylated genes and among the 5 top candidates (*GULP1*, *CLIP4*, *BAMBI*, *NT5E*, *TGFB2*), we performed extended studies of *GULP1*. In a training set, we identified *GULP1* methylation in 21/61(34%) of cases with 100% specificity. In an independent cohort, the observed methylation was 40% (146/365) in OC, 12.5% (2/16) in borderline tumors, 11% (2/18) in cystadenoma and 0% (0/13) in normal ovarian epithelium samples. *GULP1* methylation was associated with clinicopathological parameters such as stage III/IV (p=0.001), poorly differentiated grade (p=0.033), residual disease (p<0.0003), worse overall (p=0.02) and disease specific survival (p=0.01). Depletion of GULP1 in OC cells led to increased pro-survival signaling, inducing survival and colony formation, whereas reconstitution of GULP1 negated these effects, suggesting that GULP1 is required for maintaining cellular growth control.

**Keywords**: GULP1, Ovarian Cancer, Epigenetics, Biomarkers, DNA methylation

## 1. INTRODUCTION

Ovarian cancer (OC) was estimated to represent 22,240 new cases in 2018 in the United States, leading to 14,070 deaths [1]. Advances in molecular biology have revealed that genetics alone cannot explain the pervasive changes in gene expression profile of sporadic cancers. Other molecular changes, such as epigenetic abnormalities, are also recognized to have an impact on gene expression and tumorigenesis. The potential reversibility of epigenetic mechanisms make them attractive targets for the prevention, diagnosis and treatment of cancer. Numerous approaches have been undertaken to assess the OC methylome [2, 3] and to provide new targets for further studies. Moreover, although aberrant promoter methylation patterns of specific genes in ovarian tumor cells were previously demonstrated in several studies [4-7], to date, no reliable markers with clinical utility have been identified. Therefore, a better understanding of the epigenetic mechanisms responsible for OC initiation and progression is imperative for an improved management of this disease.

DNA methylation, the most studied epigenetic change in cancer, refers to the addition of a methyl group to the cytosine ring to form a methyl cytosine, but only on cytosines that precede a guanosine in the DNA sequence (CpG dinucleotide). CpG islands frequently span the promoter/regulatory region of genes with tumor suppressor activity and are usually unmethylated in normal cells [8]. The human genome in normal cells is not methylated uniformly, containing unmethylated segments interspersed with methylated regions, whereas in cancer cells, methylation patterns are altered, undergoing global DNA hypomethylation, as well as hypermethylation of CpG islands in the selected promoters/regulatory regions [9]. Aberrant promoter methylation induces gene silencing, a common phenomenon in human cancer cells and likely one of the earliest events in carcinogenesis [9-13]. The discovery of OC-specific

methylated genes that are correlated with down-regulation of expression could lead to the identification of potential biomarker candidates for risk assessment, prognosis and early detection of OC. Moreover, deciphering molecular pathways that may be deregulated due to the inactivation of a given gene by methylation may reveal novel targets for potential therapeutic interventions.

To comprehensively understand the methylation alterations in ovarian cancer, we undertook an integrated approach that consisted of identification of genome-wide expression patterns of primary OC samples and normal ovarian surface epithelium along with a pharmacologic unmasking strategy using cell lines. This comprehensive approach coupled with an innovative computational analysis led to the discovery of novel OC-specific epigenetically silenced genes. Here, we focused on the engulfment gene *GULP1* and report its aberrant silencing by methylation in multiple cohorts of primary OC samples, and its tumor suppressor activity. Our current data hypothesize that silencing of GULP1 by methylation plays an important role in ovarian carcinogenesis, playing a role in pro-survival and anti-apoptotic pathways.

## 2. MATERIALS AND METHODS

### Cell lines

Normal ovarian cell lines *OSE2A, OSE2B* and *OSE7* (kindly provided by Dr. Ie-Ming Shih - Johns Hopkins University), were maintained in the DMEM F12 medium containing 10% Fetal Bovine Serum (FBS), penicillin (100 units/mL) and streptomycin (100 μg/mL). OC cell lines *IGROV, A2780* and *2008* (kindly provided by Dr. Stephen B Howell - University of California, San Diego, CA) were maintained in RPMI1640 medium containing either 10% FBS (*IGROV, A2780*) or 5% FBS (*2008*), penicillin (100 units/mL) and streptomycin (100 μg/mL). All cells were incubated at 37°C with 5% CO2.

### 5-aza-2'-deoxycytidine (5-aza-dC) and histone deacetylase inhibitor trichostatin A (TSA) treatment

2 x $10^5$ cells of each cell line were seeded on day 0, 24 h prior to 5-aza-dC treatment (5 mol/L; Sigma). Media were changed every 24 hours with fresh 5-aza-dC and the treatment continued for 5 to 7 days. The treatment with TSA (Sigma-Aldrich, USA) was performed for the last 24 hours. Cells were harvested following completion of treatment and RNA, DNA and protein were extracted. Phosphate buffer saline (PBS) alone was used as a control. Experiments were performed in triplicates and in independent days. Stock solutions of 5-aza-dC and TSA were dissolved in PBS (pH 7.5) and 100% ethanol and subsequently diluted in PBS, respectively.

### Tissue samples

Approval for research on human subjects was obtained from The Johns Hopkins University institutional review boards. For samples collection, processing and distribution; IRB guidelines

were followed at each of the involved institutions. Detailed clinicopathological parameters for all samples used in this study are summarized in **Supplemental Table 1, Table 1 (A, B)** and Supplemental Methods.

**RNA extraction, cDNA synthesis and Reverse Transcription-PCR (RT-PCR)**

RNA extraction and cDNA conversion were performed by Qiazol reagent and Quantitect Reverse Transcription Kit (Qiagen, Valencia, CA) respectively following manufacturer instruction.

More details in Supplemental Methods.

**DNA extraction**

After microdissection, DNA was extracted using the standard phenol-chloroform extraction protocol as described previously [11]. More details in Supplemental Methods.

**Gene expression microarrays**

mRNA isolation, labeling, hybridization, and quality control were carried out as previously described [12]. Briefly, 6μg of total RNA was biotin-labeled according to the manufacturer' protocol (One Cycle Target Labeling Kit; Affymetrix) and hybridized on Affymetrix GeneChip Human Genome U133A2.0, containing probes for over 18,400 transcripts. Hybridized arrays were stained and washed on a GeneChip Fluidics Station 450 and then scanned on a GeneChip Scanner 3000. Probe detection calls were computed from the raw array data using the Affymetrix GeneChip Operating Software (GCOS). Raw data processed using Robust Multi-Averaging

(RMA) algorithm and Affymetrix Expression Console software [14]. More details in Supplemental Methods.

**Microarray data analysis**

Unsupervised clustering and gene expression data by principal component analysis was performed with the use of R2.8.2 statistical software and GenePattern software (http://www.broad.mit.edu/cancer/software/genepattern/). Supervised analysis of methylation data were carried out with a moderated *t* test with Benjamini-Hochberg correction algorithm with a significance level of *P* less than .001 and an absolute difference in methylation greater than 1.5 between the means of the 2 populations to increase the likelihood of detecting biologically significant changes in methylation levels. Detailed bioinformatics analysis procedures are available in the supplementary method section.

**Sodium Bisulfite Treatment and Sequencing**

EpiTect Bisulfite kit (QIAGEN Inc., Valencia, CA) or the EZ DNA methylation kit (Zymogen, BaseClear, Leiden, the Netherlands) were used. After treatment, DNA was stored at −80°C until used. Bisulfite Sequencing primer sets are available in **Supplemental Table 3B**. More details in Supplemental Methods.

**Conventional and Quantitative Methylation specific PCR (QMSP)**

Specific primers for methylated or unmethylated templates were designed to amplify the most differentially methylated CGs observed by bisulfite sequencing on the “promoter” region of *GULP1*. For **QMSP,** a probe has been designed within the amplified area that includes several

CGs sites. Bisulfite-modified DNA was used as a template for MSP and QMSP, as previously described [15]. The primers/probe sequences and PCR condition for MSP/QMSP and RT-PCR for GULP1 are available in **Supplemental Table 2, 3**. Detailed explanation available in Supplemental Methods.

**Antibodies and immunoblot analysis**

We obtained *GULP1* antibody from Novus, Littleton, CO and *ACTB* from Abcam, Cambridge, MA. All other antibodies (pAKT, total AKT, pPDK1, total PDK1, pPTEN, total PTEN, mTOR, cyclinD1, pEGFR, pSTAT3, total STAT3, β-catenin, and α-GFP) were purchased from Cell Signaling (Beverly, MA).

**Plasmid constructs**

Expression vector for *GULP1* (pCMV6-AC-*GULP1*-GFP), control vector (pCMV6-AC-GFP) and knock-down shRNA sequence (5'-GAGAATAACTCAAGTATCAGCACCTCCAG-3') and its negative control were purchased from OriGene (Rockville, MD). Lentiviral vector pLenti-GULP1-C-mGFP and empty control were obtained from OriGene.

**Lentiviral infection**

Lentivirus were amplified by transfecting HEK293T cells with the packaging plasmids (Lenti-vpak packaging kit, OriGene) as per manufacturer's instructions. More details available in Supplemental Methods.

**RNA interference**

Four unique GULP1 shRNA clones, empty vector or scramble shRNA were obtained from OriGene (Rockville, MD). To deplete target gene expression four independent GULP1 shRNA clones were pooled together and transiently transfected into the A2780 cells using Lipofectamine RNAiMAX (Invitrogen, Grand Island, NY) following manufacturer's instructions. More details in Supplemental Methods.

**Cell viability/growth assay**

Please see supplementary methods.

**Colony formation assay**

Cell lines were seeded in 10 cm dishes and transfected with *GULP1* expression vector (pCMV6-AC-*GULP1*-GFP) and empty vector (pCMV6-AC-GFP). Cells were cultured for 2 weeks in medium containing 400 µg/mL of G418 (Cellgro, Manassas, VA). After 2 weeks, cells were washed twice with PBS, fixed with 25% acetic acid and 75% methanol at room temperature for 10 mins and then stained with 0.1% crystal violet. Colonies were counted and the number of colonies per dish was averaged from three independent experiments. *GULP1* expression was confirmed by western blotting, 48 hours after transfection.

**Invasion assay**

$2.5x10^4$ of the *GULP1* transfected cells were seeded into the upper compartment of the invasion chamber containing 500 µl of serum-free medium in 24 well BioCoat Matrigel Invasion

Chambers (8 μm pore size; BD Biosciences, USA)] whereas the lower chamber containing 750 μl of RPMI-1640 medium with 10% FBS as a chemoattractant. After 72 hours of incubation in a humidified atmosphere containing 5% $CO_2$ at 37°C, the non-invading cells were removed from the upper surface of the membrane by a cotton swab. The membranes were then fixed with methanol and stained with Hematoxylin and Eosin. Invading cells were photographed and counted in three random non-overlapping fields under a light microscope.

**Expression data processing for pathway analysis**

Raw RNA-Seq data was retrieved from publicly available TCGA databases. RNA-Seq or internally generated microarray data preprocessing and normalization steps were performed in R version 3.1.0 using DEseq package from Bioconductor. The resulting matrix contained mRNA expression information for over 20K genes across all analyzed samples. Normalized gene expression data were loaded into iPANDA [16]. The software enables calculation of the Pathway Activation Score (PAS) for each of the 374 pathways analyzed, a value which serves as a quantitative measure of differential pathway activation. A collection of 374 intracellular signaling pathways (which cover a total of 2,294 unique genes) strongly implicated with various solid malignancies was obtained from the SABiosciences (http://www.sabiosciences.com/pathwaycentral.php), and used for the computational algorithm as described previously [16-18].

**Statistical analysis**

Statistical analysis was performed with IBM SPSS Statistics 19.0 (SPSS Inc., Chicago, IL). The cut-off value for *GULP1* methylation was determined in the training set using ROC by

maximizing sensitivity and specificity. The same cut-off value was employed for the independent test set. Differences in methylation between normal and cancer were calculated using the Fishers exact or Pearson's chi-square test or Mann-Whitney U test. Associations between the presence of hypermethylation and clinicopathological characteristics were assessed in logistic regression models, where hypermethylation was used as dependent factor and the clinicopathological characteristics were used as independent factors. Overall survival (OS) was defined as the time from diagnosis to death of any cause or last follow-up visit alive. Disease specific survival (DSS) was defined as the time from diagnosis to death of OC or last follow-up visit alive. Differences in OS and DSS according to clinicopathological characteristics and methylation of GULP1 were analyzed using Cox regression analyses. All significant variables with a *P* value <0.10 in univariate analysis were included in multivariate analysis. *P* values of <0.05 were considered statistically significant. Survival curves were generated using the Kaplan-Meier method, with evaluation of the differences by the Mantel-Cox log rank test. Methylation values were visually compared using scatter plots.

## 3. RESULTS

### Genome-wide methylation profiles of OC by the integration of pharmacologic unmasking data in cell lines and expression array data of primary OC and normal ovarian epithelium samples

We conducted an Affymetrix microarray analysis on 15 late stage primary OC samples, 10 normal ovarian surface epithelium brushing of tumor-free female patients, 3 immortalized normal ovarian cell lines (OSE2A, OSE2B and OSE7) and 3 OC cell-lines (IGROV, A2780 and 2008). All cell lines were treated with 5-aza-dC.

A linear regression model (false discovery rate = 0.05) using all the data set identified 5718 probes differentially downregulated in cancer samples compared to healthy controls and 4870 probes significantly downregulated in tumor cell lines compared to the normal cells. To identify highly relevant OC-specific methylated genes, the following selection criteria were employed in a sequential fashion: *a)* genes with low expression in primary tumor samples but expressed in normal ovarian surface epithelium samples , *b)* genes with low expression in cancer cell lines but expressed in normal cell lines *c)* genes that have a low expression level in primary tumor tissue and cancer cell lines in comparison with normal ovarian epithelium and cell lines, *d)* genes reactivated in cancer cell lines by 5-aza-dC treatment. All these criteria were combined using a score scheme methodology and the top 250 probes, corresponding to 88 genes, were selected for further analysis. Additional filtering scheme was employed as shown in **Figure 1**, resulting in a total of 43 genes that were downregulated in tumor samples (or cancer cell lines) and reactivated after treatment with 5-aza-dC (**Supplemental Table 2**).

**Experimental validation of methylated genes identified by array-based analysis**

43 candidate genes (summarized in **Supplemental Table 2**) were analyzed by bisulfite sequencing in the same cell-lines used for pharmacologic unmasking. Five of the 43 genes (*GULP1, CLIP4, BAMBI, NT5E, TGFB2*) showed a cancer-specific methylation pattern. As *GULP1* was reported to be involved in ovarian carcinogenesis [19] , we focused on evaluating *GULP1* methylation in different cohorts of primary OC samples. We also performed functional characterization of *GULP1* in ovarian carcinogenesis.

**Methylation analysis of *GULP1* in OC and normal ovarian epithelium by conventional MSP**

Based on our bisulfite sequencing data (**Figure 2A, left**), we designed MSP primers to assess the methylation status of *GULP1* by PCR. After optimizing MSP primers using cell lines **(Figure 2A, right)**, we analyzed 15 primary OC and 13 normal ovarian epithelial tissue samples. Methylation of *GULP1*was determined in 15/15 (100%) tumor tissues and low level of methylation was detected in 3/13 (23%) ($p<0.0001$) normal ovarian epithetlium specimens **(Figure 2B)**.

***GULP1* methylation inversely correlates with mRNA and protein expression levels**

We observed low level of *GULP1* expression in ovarian tumors in comparison with normal ovarian surface epithelial washing samples by microarray analysis (**Figure 2C**). To assess the association between methylation of *GULP1* and its expression, we measured mRNA and protein expression of *GULP1* in normal ovarian and cancer cell-lines. We observed an inverse

correlation between *GULP1* expression and methylation in all cell lines analyzed (**Figure 2A and D**). OC cell lines (2008 and IGROV) that harbor *GULP1* methylation were treated with either 5-aza-dC or TSA, and *GULP1* re-expression was observed only by 5-aza-dC treatment but not by TSA (**Supplemental Figure 1A and data not shown**). This observation is complemented by the data that shows the inverse correlation between expression and methylation in primary ovarian tumors as well (**Supplemental Figure 1B**), suggesting that *GULP1* methylation is an important regulatory mechanism for its expression.

To further validate our observations of *GULP1* expression and methylation in a large-scale population-based dataset, we used gene expression and methylation data available for *GULP1* in the The Cancer Genome Atlas (TCGA) ovarian serous cohort. Confirming our findings, expression of *GULP1* was significantly lower in tumor samples (n=569) compared to tissue specific normal controls (n=8), (p=0.0001) (**Figure 2 E**). We next categorized *GULP1* mRNA expression as high level (one standard deviation above the mean of the TCGA tumor group; n=83) or low level (one standard deviation below the mean of the TCGA tumor group; n=16) (**Figure 2F**). *GULP1* was significantly more hypermethylated in tumors with low *GULP1* expression levels (**Figure 2 G**), reinforcing that *GULP1* methylation in OC is associated with expression.

**QMSP for *GULP1* methylation in two independent sets of ovarian tissue samples**

We tested two independent cohorts of primary ovarian tumor tissue samples. In the training set, we used QMSP on 61 OC samples and 13 normal ovarian epithelium samples. Using a methylation cutoff value of 0.72, 34.4% (21/61) of the tumor samples were found to be hypermethylated in comparison to 0% (0/13) of the normal ovarian samples (p=0.03) (**Figure**

**3A**). The cutoff of 0.72 was obtained by maximizing sensitivity and specificity. By two methods, we obtained the same value of the cutoff. By considering it above the highest normal and by using ROC (receiver operating curve) to pinpoint the intersection of highest sensitivity and specificity. In the independent validation cohort (**Table 1 B**, **Supplemental Table 1)**, the sensitivity and specificity of *GULP1* methylation was 40% and 100% respectively, considering the same cutoff of 0.72. The observed methylation frequencies were 146/365 (40%), 2/18 (11%) and 2/16 (13%) for OC, borderline tumors and cystadenomas respectively (**Figure 3B**).

**Association of *GULP1* methylation with clinicopathological parameters**

We examined associations between several clinicopathological and demographic parameters with methylation of *GULP1* in our clinical cohort of 365 ovarian tumor samples. By logistic regression analysis, *GULP1* methylation was associated with older age ($p \leq 0.006$), serous histology ($p=0.033$), higher grade ($p=0.033$), advanced stage III/IV ($p=0.001$) and residual disease (> 2cm) ($p \leq 0.0003$) (**Table 1C**, **Figure 3C-E**).

We further evaluated *GULP1* methylation and patient's outcome. The median follow-up was 29 months (range 0-234). As shown by Kaplan–Meier survival curves, using cox regression analysis, *GULP1* methylation was significantly associated with worse OS ($p=0.023$) and disease specific survival (DSS) ($p=0.011$) (**Figure 3F, G**). In multivariate analysis both OS and DSS, higher age, higher stage and presence of residual disease after surgery, but not *GULP1* methylation, were predictive of poor prognosis (data not shown).

Since our validation cohort comprised of patients with different histologic subtypes of OC, we evaluated the association between *GULP1* methylation and clinicopathological parameters in patients with serous OC (n=222), which represents the most common type of epithelial OC [20].

Similarly, *GULP1* methylation was significantly higher in serous OC samples compared to normal controls, borderline tumors ($p<0.001$) and cystadenomas ($p=0.002$) (data not shown).

***GULP1* modulates ovarian cancer cell viability and colony formation**

To test the role of *GULP1* in cell growth and proliferation, we overexpressed *GULP1* in IGROV OC cell line. Forced expression of *GULP1* resulted in decreased cell survival of IGROV cells ($p=0.002$) **(Figure 4A, B, Supplemental Figure 1C)**. Moreover, down-regulation of the proliferative marker *Cyclin D1* in *GULP1*-overexpressing cells is consistent with the decrease in cell viability. The opposite effect on cell viability was observed after *GULP1* expression knock-down in A2780 cells, compared to control and scramble transfection ($p=0.0001$) **(Figure 4C, D).** To assess long-term growth, colony formation assays were performed. *GULP1* overexpression in 2008 cells showed a potent growth-suppressive activity by markedly reducing the number and size of the colonies ($p=0.03$) (**Figure 4E**). In an invasion assay, we found that the number of invasive 2008 cells decreased after 48 h of *GULP1* transfection ($p=0.04$) (**Figure 4F**). As expected, a significant reduction in cell viability was also observed in *GULP1* expressing cells (**Figure 4G**). Collectively, these findings suggest that *GULP1* exhibits a growth inhibitory ability.

***GULP1* expression correlates with dysregulation of cancer promoting pathways**

To explore the potential signaling pathways that may be associated with *GULP1* expression in cancer, we analyzed Affymetrix microarray gene expression data obtained from 15 OCs and 10 normal ovarian epithelium samples by two independent computational approaches [Ingenuity Pathway Analysis (IPA) and iPANDA [16]]. The deregulated pathways by both approaches are shown in **Supp. Figure 2A and 2B**. Notably, WNT signaling was among the most significantly

dysregulated pathways identified by both bioinformatics approaches. To experimentally validate this observation, we performed western blot analysis of β-catenin, a downstream effector of WNT activation [21], in two cell lines that exhibit no endogenous *GULP1* expression and one cell line that expresses *GULP1*. The level of β-catenin was substantially lower in *GULP1* expressing cells compared to *GULP1* non-expressing cells (**Supp. Figure 2C**). Furthermore, the phosphorylation of multifunctional serine/threonine kinase *GSK3*, which targets β-catenin for ubiquitination and subsequent proteasomal degradation [21], was much higher in *GULP1* expressing cells (**Supp. Figure 2C**), suggesting that *GULP1* may regulate WNT/β-catenin signaling pathway in ovarian tumorigenesis.

We then analyzed RNA-sequencing data from TCGA OC dataset (n=569). We categorized *GULP1* mRNA expression as high level (n=83) or low level (n=16), and used iPANDA to predict differentially activated pathways in these tumor cohorts. Our analysis revealed that pathways involved in cancer initiation, progression and maintenance (such as those associated with AKT, ILK, RAS, MAPK/ERK, PAK/P38, and WNT signaling) were significantly upregulated in most of the patients in *GULP1*-low expression group, whereas pathways associated with apoptosis have been significantly down-regulated in this cohort (**Figure 5A**). Interestingly, a pattern of dysregulated signaling pathways observed in *GULP1*-low expressing TCGA tumors was very similar to that seen in 15 OCs in our data set (**Supp. Figure 2B**). Taken together, these findings suggest that *GULP1* regulates genes associated with key cancer pathways and may act as a potential tumor suppressor in OC.

**Validation of pro-survival signaling pathways**

Forced *GULP1* expression in IGROV cell line led to a noticeably lower MAPK, AKT and PDK1 (the upstream activator of AKT) phosphorylation (**Figure 5B**) which is paralleled with a significant decrease in cell viability after forced *GULP1* expression (**Figure 4B**). To further confirm the role of *GULP1* in the regulation of the AKT activation, we used *GULP1*-specific shRNA to selectively knock-down its expression in A2780 cell line. As expected, *GULP1* knock-down significantly increase in AKT and MAPK activation (**Figure 5C**). These results paralleled a significant increase in viability of *GULP1*-depleted A2780 cells (**Figure 4D**). Taken together with pathway activation analyses, our data suggest that *GULP1* regulates cellular survival and proliferation by modulating key cancer-associated pathways.

## 4. DISCUSSION

Numerous strategies using different platforms have been undertaken to identify cancer-specific methylated genes. We employed a genome-wide microarray platform using a carefully selected cohort of normal and OC tissues/cell lines, coupled with functional pharmacologic unmasking of epigenetically silenced genes by treating cancer cell lines with a demethylating agent. We identified 43 novel potentially OC specific methylated genes by computational approach and additional filtering criteria, and 5 genes (*CLIP4, NT5E, BAMBI, TGFB2, and GULP1*) were experimentally validated to be regulated by methylation in this tumor type.

The biological role of these potential tumor suppressor genes (TSGs) in the initiation and progression of OC is largely unknown. A previous report suggested that *CLIP4* regulates receptor tyrosine kinase endocytosis and controls growth factor-induced cellular functions [22], whereas mutations in *NT5E* have been shown in calcification of joints and arteries [23]. Downregulation of *BAMBI*, a regulator of the transforming growth factor-beta (TGF-β) signaling pathway, was reported in lung, bladder and breast cancer [24-26]. However, contrasting data were reported in OC [27] and its role in OC warrants further investigation. *TGFB2* is frequently upregulated in several neoplasms [28-30], however the effect of *TGFB2* expression on clinical outcome remains controversial [29, 31, 32]. While one study reported *TGFB2* overexpression in OCs [28], its role in ovarian tumorigenesis is poorly understood. Expression of *GULP1*, a critical gene in the engulfment pathway, was reported to positively regulate TGF-β signaling, leading to growth inhibition of OC cell lines [19]. Moreover, its expression was shown to be frequently down-regulated in a small cohort of ovarian adenocarcinomas [19]. This prompted us to perform methylation analysis of *GULP1* in numerous primary ovarian tumor tissues and cell lines and also to functionally characterize this gene. In all the three data sets we have analyzed, *GULP1*

methylation was found to be OC specific. Our findings indicate that in at least one third of OC cases, *GULP1* is inactivated by methylation. Furthermore, array based data and RT-PCR analysis confirmed the reactivation of *GULP1* in cell lines following the 5-aza-dC treatment. Inverse correlation of *GULP1* methylation with expression was also observed in the TCGA data set, further validating our findings.

*GULP1* methylation was correlated with late stage OC, which is in line with previously reported methylation markers in advanced stages of OC [33], highlighting its potential as a prognostic marker after further validation. *GULP1* methylation was seen in 26% of patients with early stage (stage I and II) disease, suggesting that *GULP1* silencing by methylation may be an early event in some ovarian tumors. *GULP1* methylation was significantly higher in serous ovarian carcinoma and additional studies are needed to confirm *GULP1* serous histology specificity in OC. *GULP1* methylation levels in cystadenomas and borderline ovarian tumor samples fall between that of normal and OC specimens. Only a few reports are available about gene methylation in cystadenomas and borderline tumors. Tam et al. [34] showed a similar trend of methylation in a panel of genes in these ovarian neoplasms.

Our data showed that *GULP1* methylation is associated with late stage, residual disease and high grade These were observed by univariate analysis, but not in multivariate analysis, indicating that it is not an independent factor. A study with a larger cohort is needed to explore and confirm *GULP1* methylation as a valuable clinical tool for patient prognosis at the time of diagnosis. Perhaps other yet to be identified (or known) prognostic factors could be combined with *GULP1* methylation status to better predict patient prognosis. Interestingly, although not statistically significant, early stage patients with *GULP1* methylation, had a trend towards worse prognosis. Multiple data sets with well-annotated follow-up data need to be tested to determine

whether *GULP1* methylation can be used as a prognostic factor independently or in combination with others.

*GULP1* is a cytoplasmic adaptor protein composed of a phosphotyrosine binding (PTB) domain at its N terminus, and a C-terminal serine/proline-rich region [35, 36]. Several PTB domain-containing proteins, act as adaptor molecules, binding to phosphorylated tyrosine residues present on activated receptors, and recruiting downstream molecules to form a signaling complex [37]. Although *GULP1* downregulation in OCs was previously reported in a small cohort [19], the multifaceted molecular mechanisms underlying this association is not yet defined. Besides its well characterized primary function in engulfment [35], *GULP1* plays a role in the process of programmed cell death [38-40], lipid homeostasis [41] and regulation of *Arf6*-mediated signaling, a GTPase known to regulate multiple cellular processes including endocytosis, secretion, phagocytosis, cell adhesion and cell migration [42]. More recently, *GULP1* was established as a novel downstream regulator of TGF-β signaling in ovarian cells, crucial for maintaining their sensitivity toward TGF-β-induced cell growth arrest [19]. Our studies have shed light on the mechanisms underlying *GULP1*-mediated growth suppression. The novel bioinformatics software suite used for the analysis of intracellular signaling pathway activation using transcriptomic data, for quantitative and qualitative comparison of the signaling pathway activation between *GULP1*-low-expressing and *GULP1*-high ovarian tumors in TCGA-OC dataset, has predicted that mitogenic and survival signaling pathways, such as AKT, MAPK/ERK, RAS, ILK, PAK/P38, WNT and JNK were significantly upregulated among *GULP1*-low tumors. These pro-survival signaling axes play a crucial role in cancer initiation, progression and maintenance in various solid tumors, including OC, and may contribute to acquisition of an aggressive phenotype via inhibition of apoptosis and induction of cell

proliferation. In line with these observations, pro-apoptotic and anti-proliferative pathways including those associated with TP53 and TGF-β signaling were predicted to be downregulated in most of the *GULP1*-low tumors. *Of note*, in the low-*GULP1* cohort, TGF-β signaling was significantly down-regulated in 12 of 16 patients, consistent with the role of *GULP1* in mediating the anti-proliferative effect of TGF-β [19]. In accordance with the *in-silico* analysis, reconstitution of *GULP1* expression *in vitro* resulted in marked suppression of MAPK and AKT phosphorylation, along with concomitant reduction in cell proliferation, survival and invasion, while *GULP1* depletion led to opposite effects. Although our findings indicate that GULP1 may assert its tumor suppressive activities by tethering members of multiple, cross-talking pathways involved in cell growth and survival control, further biological studies are warranted to fully elucidate the role of GULP1 in ovarian tumorigenesis.

In summary, by an integrated approach, we reported the identification of several novel OC specific methylated genes. Among these genes, *GULP1* gene was tested in a training set and further validated in a larger cohort of ovarian samples. Our data implicate that epigenetic regulation of *GULP1* expression may play an important role in OC pathogenesis, and suggests its potential clinical value as a promising prognostic biomarker. Although we did not investigate other possible mechanisms for *GULP1* down-regulation, which may include microRNA–mediated silencing, transcriptional regulation, or homozygous deletions, a deeper understanding of the role of *GULP1* methylation in the development of OC may offer additional possibilities for the management of OC.

**ACKNOWLEDGMENTS**

We thank Dr. Richard Roden/ Dr. T.C. Wu –Johns Hopkins University for kindly providing us with 15 ovarian cancer frozen samples. We thank Dr. Birrer (and his team - NCI) for the microarray data on 10 normal ovarian brushing samples from patients without ovarian cancer (normal Epithelium Brushings). We thank Jacqueline C. Junn, Juna Lee, Luciane T. Kagohara and Christina Michailidi for technical assistance.

**FUNDING**

This work was supported by a career development award to M. O. Hoque from Specialized Program of Research Excellence and P50 CA098252 (T-C Wu) National Institutes of Health (NIH)/National Cancer Institute (NCI). The funders had no role in study design, data collection and analysis, decision to publish, or preparation of the manuscript.

**Conflict of interest**: None

## REFERENCES

[1] R.L. Siegel, K.D. Miller, A. Jemal, Cancer Statistics, 2018, Ca-Cancer J Clin, 68 (2018) 7-30.
[2] N. Cancer Genome Atlas Research, Integrated genomic analyses of ovarian carcinoma, Nature, 474 (2011) 609-615.
[3] T. Witte, C. Plass, C. Gerhauser, Pan-cancer patterns of DNA methylation, Genome Med, 6 (2014) 66.
[4] D. Pils, P. Horak, P. Vanhara, M. Anees, M. Petz, A. Alfanz, A. Gugerell, M. Wittinger, A. Gleiss, V. Auner, D. Tong, R. Zeillinger, E.I. Braicu, J. Sehouli, M. Krainer, Methylation status of TUSC3 is a prognostic factor in ovarian cancer, Cancer, 119 (2013) 946-954.
[5] S.H. Wei, C. Balch, H.H. Paik, Y.S. Kim, R.L. Baldwin, S. Liyanarachchi, L. Li, Z. Wang, J.C. Wan, R.V. Davuluri, B.Y. Karlan, G. Gifford, R. Brown, S. Kim, T.H. Huang, K.P. Nephew, Prognostic DNA methylation biomarkers in ovarian cancer, Clinical cancer research : an official journal of the American Association for Cancer Research, 12 (2006) 2788-2794.
[6] M. Campan, M. Moffitt, S. Houshdaran, H. Shen, M. Widschwendter, G. Daxenbichler, T. Long, C. Marth, I.A. Laird-Offringa, M.F. Press, L. Dubeau, K.D. Siegmund, A.H. Wu, S. Groshen, U. Chandavarkar, L.D. Roman, A. Berchuck, C.L. Pearce, P.W. Laird, Genome-scale screen for DNA methylation-based detection markers for ovarian cancer, PloS one, 6 (2011) e28141.
[7] B.S. Gloss, K.I. Patterson, C.A. Barton, M. Gonzalez, J.P. Scurry, N.F. Hacker, R.L. Sutherland, P.M. O'Brien, S.J. Clark, Integrative genome-wide expression and promoter DNA methylation profiling identifies a potential novel panel of ovarian cancer epigenetic biomarkers, Cancer letters, 318 (2012) 76-85.
[8] J. Sandoval, M. Esteller, Cancer epigenomics: beyond genomics, Curr Opin Genet Dev, 22 (2012) 50-55.
[9] J.G. Herman, S.B. Baylin, Gene silencing in cancer in association with promoter hypermethylation, N Engl J Med, 349 (2003) 2042-2054.
[10] P.A. Jones, S.B. Baylin, The fundamental role of epigenetic events in cancer, Nat Rev Genet, 3 (2002) 415-428.
[11] M. Brait, S. Begum, A.L. Carvalho, S. Dasgupta, A.L. Vettore, B. Czerniak, O.L. Caballero, W.H. Westra, D. Sidransky, M.O. Hoque, Aberrant promoter methylation of multiple genes during pathogenesis of bladder cancer, Cancer Epidemiol Biomarkers Prev, 17 (2008) 2786-2794.
[12] M.O. Hoque, M.S. Kim, K.L. Ostrow, J. Liu, G.B. Wisman, H.L. Park, M.L. Poeta, C. Jeronimo, R. Henrique, A. Lendvai, E. Schuuring, S. Begum, E. Rosenbaum, M. Ongenaert, K. Yamashita, J. Califano, W. Westra, A.G. van der Zee, W. Van Criekinge, D. Sidransky, Genome-wide promoter analysis uncovers portions of the cancer methylome, Cancer Res, 68 (2008) 2661-2670.
[13] M. Brait, M. Loyo, E. Rosenbaum, K.L. Ostrow, A. Markova, S. Papagerakis, M. Zahurak, S.M. Goodman, M. Zeiger, D. Sidransky, C.B. Umbricht, M.O. Hoque, Correlation between BRAF mutation and promoter methylation of TIMP3, RARbeta2 and RASSF1A in thyroid cancer, Epigenetics, 7 (2012) 710-719.
[14] N.C.f.B. Information., G.E.O. database., http://ncbi.nlm.nih.gov/geo. , (Accessed December 1,
2009).

[15] J.G. Herman, J.R. Graff, S. Myohanen, B.D. Nelkin, S.B. Baylin, Methylation-specific PCR: a novel PCR assay for methylation status of CpG islands, Proc Natl Acad Sci U S A, 93 (1996) 9821-9826.
[16] I.V. Ozerov, K.V. Lezhnina, E. Izumchenko, A.V. Artemov, S. Medintsev, Q. Vanhaelen, A. Aliper, J. Vijg, A.N. Osipov, I. Labat, M.D. West, A. Buzdin, C.R. Cantor, Y. Nikolsky, N. Borisov, I. Irincheeva, E. Khokhlovich, D. Sidransky, M.L. Camargo, A. Zhavoronkov, In silico Pathway Activation Network Decomposition Analysis (iPANDA) as a method for biomarker development, Nat Commun, 7 (2016) 13427.
[17] A.A. Buzdin, A.A. Zhavoronkov, M.B. Korzinkin, S.A. Roumiantsev, A.M. Aliper, L.S. Venkova, P.Y. Smirnov, N.M. Borisov, The OncoFinder algorithm for minimizing the errors introduced by the high-throughput methods of transcriptome analysis, Front Mol Biosci, 1 (2014) 8.
[18] N.M. Borisov, N.V. Terekhanova, A.M. Aliper, L.S. Venkova, P.Y. Smirnov, S. Roumiantsev, M.B. Korzinkin, A.A. Zhavoronkov, A.A. Buzdin, Signaling pathway activation profiles make better markers of cancer than expression of individual genes, Oncotarget, (2014).
[19] C.I. Ma, C. Martin, Z. Ma, A. Hafiane, M. Dai, J.J. Lebrun, R.S. Kiss, Engulfment protein GULP is regulator of transforming growth factor-beta response in ovarian cells, J Biol Chem, 287 (2012) 20636-20651.
[20] S.A. Cannistra, Cancer of the ovary, N Engl J Med, 351 (2004) 2519-2529.
[21] B.T. MacDonald, K. Tamai, X. He, Wnt/beta-catenin signaling: components, mechanisms, and diseases, Dev Cell, 17 (2009) 9-26.
[22] K. Kowanetz, N. Crosetto, K. Haglund, M.H. Schmidt, C.H. Heldin, I. Dikic, Suppressors of T-cell receptor signaling Sts-1 and Sts-2 bind to Cbl and inhibit endocytosis of receptor tyrosine kinases, J Biol Chem, 279 (2004) 32786-32795.
[23] C. St Hilaire, S.G. Ziegler, T.C. Markello, A. Brusco, C. Groden, F. Gill, H. Carlson-Donohoe, R.J. Lederman, M.Y. Chen, D. Yang, M.P. Siegenthaler, C. Arduino, C. Mancini, B. Freudenthal, H.C. Stanescu, A.A. Zdebik, R.K. Chaganti, R.L. Nussbaum, R. Kleta, W.A. Gahl, M. Boehm, NT5E mutations and arterial calcifications, N Engl J Med, 364 (2011) 432-442.
[24] S. Marwitz, S. Depner, D. Dvornikov, R. Merkle, M. Szczygiel, K. Muller-Decker, P. Lucarelli, M. Wasch, H. Mairbaurl, K.F. Rabe, C. Kugler, E. Vollmer, M. Reck, S. Scheufele, M. Kroger, O. Ammerpohl, R. Siebert, T. Goldmann, U. Klingmuller, Downregulation of the TGFbeta Pseudoreceptor BAMBI in Non-Small Cell Lung Cancer Enhances TGFbeta Signaling and Invasion, Cancer research, 76 (2016) 3785-3801.
[25] S.S. Khin, R. Kitazawa, N. Win, T.T. Aye, K. Mori, T. Kondo, S. Kitazawa, BAMBI gene is epigenetically silenced in subset of high-grade bladder cancer, International journal of cancer, 125 (2009) 328-338.
[26] D.S. Lang, S. Marwitz, U. Heilenkotter, W. Schumm, O. Behrens, R. Simon, M. Reck, E. Vollmer, T. Goldmann, Transforming growth factor-beta signaling leads to uPA/PAI-1 activation and metastasis: a study on human breast cancer tissues, Pathology oncology research : POR, 20 (2014) 727-732.
[27] D. Pils, M. Wittinger, M. Petz, A. Gugerell, W. Gregor, A. Alfanz, R. Horvat, E.I. Braicu, J. Sehouli, R. Zeillinger, W. Mikulits, M. Krainer, BAMBI is overexpressed in ovarian cancer and co-translocates with Smads into the nucleus upon TGF-beta treatment, Gynecol Oncol, 117 (2010) 189-197.

[28] M.E. Gordinier, H.Z. Zhang, R. Patenia, L.B. Levy, E.N. Atkinson, M.A. Nash, R.L. Katz, C.D. Platsoucas, R.S. Freedman, Quantitative analysis of transforming growth factor beta 1 and 2 in ovarian carcinoma, Clin Cancer Res, 5 (1999) 2498-2505.
[29] C. Chen, K.N. Zhao, P.P. Masci, S.R. Lakhani, A. Antonsson, P.T. Simpson, L. Vitetta, TGFbeta isoforms and receptors mRNA expression in breast tumours: prognostic value and clinical implications, BMC cancer, 15 (2015) 1010.
[30] H. Friess, Y. Yamanaka, M. Buchler, M. Ebert, H.G. Beger, L.I. Gold, M. Korc, Enhanced expression of transforming growth factor beta isoforms in pancreatic cancer correlates with decreased survival, Gastroenterology, 105 (1993) 1846-1856.
[31] K.H. Schlingensiepen, F. Jaschinski, S.A. Lang, C. Moser, E.K. Geissler, H.J. Schlitt, M. Kielmanowicz, A. Schneider, Transforming growth factor-beta 2 gene silencing with trabedersen (AP 12009) in pancreatic cancer, Cancer science, 102 (2011) 1193-1200.
[32] C.K. Sun, M.S. Chua, J. He, S.K. So, Suppression of glypican 3 inhibits growth of hepatocellular carcinoma cells through up-regulation of TGF-beta2, Neoplasia, 13 (2011) 735-747.
[33] R.L. Huang, F. Gu, N.B. Kirma, J. Ruan, C.L. Chen, H.C. Wang, Y.P. Liao, C.C. Chang, M.H. Yu, J.M. Pilrose, I.M. Thompson, H.C. Huang, T.H. Huang, H.C. Lai, K.P. Nephew, Comprehensive methylome analysis of ovarian tumors reveals hedgehog signaling pathway regulators as prognostic DNA methylation biomarkers, Epigenetics, 8 (2013) 624-634.
[34] K.F. Tam, V.W. Liu, S.S. Liu, P.C. Tsang, A.N. Cheung, A.M. Yip, H.Y. Ngan, Methylation profile in benign, borderline and malignant ovarian tumors, J Cancer Res Clin Oncol, 133 (2007) 331-341.
[35] E. Smits, W. Van Criekinge, G. Plaetinck, T. Bogaert, The human homologue of Caenorhabditis elegans CED-6 specifically promotes phagocytosis of apoptotic cells, Curr Biol, 9 (1999) 1351-1354.
[36] H.P. Su, E. Brugnera, W. Van Criekinge, E. Smits, M. Hengartner, T. Bogaert, K.S. Ravichandran, Identification and characterization of a dimerization domain in CED-6, an adapter protein involved in engulfment of apoptotic cells, J Biol Chem, 275 (2000) 9542-9549.
[37] Q.A. Liu, M.O. Hengartner, Candidate adaptor protein CED-6 promotes the engulfment of apoptotic cells in C. elegans, Cell, 93 (1998) 961-972.
[38] P.W. Reddien, S. Cameron, H.R. Horvitz, Phagocytosis promotes programmed cell death in C. elegans, Nature, 412 (2001) 198-202.
[39] D.J. Hoeppner, M.O. Hengartner, R. Schnabel, Engulfment genes cooperate with ced-3 to promote cell death in Caenorhabditis elegans, Nature, 412 (2001) 202-206.
[40] P.M. Mangahas, Z. Zhou, Clearance of apoptotic cells in Caenorhabditis elegans, Semin Cell Dev Biol, 16 (2005) 295-306.
[41] R.S. Kiss, Z. Ma, K. Nakada-Tsukui, E. Brugnera, G. Vassiliou, H.M. McBride, K.S. Ravichandran, Y.L. Marcel, The lipoprotein receptor-related protein-1 (LRP) adapter protein GULP mediates trafficking of the LRP ligand prosaposin, leading to sphingolipid and free cholesterol accumulation in late endosomes and impaired efflux, J Biol Chem, 281 (2006) 12081-12092.
[42] Z. Ma, Z. Nie, R. Luo, J.E. Casanova, K.S. Ravichandran, Regulation of Arf6 and ACAP1 signaling by the PTB-domain-containing adaptor protein GULP, Curr Biol, 17 (2007) 722-727.
[43] J. Monks, D. Rosner, F.J. Geske, L. Lehman, L. Hanson, M.C. Neville, V.A. Fadok, Epithelial cells as phagocytes: apoptotic epithelial cells are engulfed by mammary alveolar epithelial cells and repress inflammatory mediator release, Cell Death Differ, 12 (2005) 107-114.

[44] S.Y. Park, K.B. Kang, N. Thapa, S.Y. Kim, S.J. Lee, I.S. Kim, Requirement of adaptor protein GULP during stabilin-2-mediated cell corpse engulfment, J Biol Chem, 283 (2008) 10593-10600.
[45] S.Y. Park, S.Y. Kim, K.B. Kang, I.S. Kim, Adaptor protein GULP is involved in stabilin-1-mediated phagocytosis, Biochem Biophys Res Commun, 398 (2010) 467-472.

**Figure Legends**

**Figure 1. Filtering scheme for selection of candidate TSGs.** We used 3 immortalized normal ovarian epithelium cell lines (OSE2A, OSE2B and OSE7), 3 ovarian cancer (OC) cell-lines (IGROV, A2780 and 2008), 15 late stage primary ovarian cancer samples and 10 normal ovarian samples derived from the surface epithelium brushing of tumor-free females to screen for candidate TSGs after microarray analysis. Cell lines were treated with 5 µmol/L 5-aza-dC (reactivation filter) before microarray analysis. Combining the reactivation filters in cell lines and primary tumor tissues expression patterns, we obtained 88 unique candidate TSGs. We diminished the number of candidates by excluding 22 genes that are not promising for suitable primers design, 12 genes contain no CpG island in their promoters, 9 genes probes located outside the extended promoters/regulatory regions and 2 genes were previously reported as methylated in OC. From the remaining 43 genes, by empirical testing, we found 5 genes that harbored cancer specific hypermethylation in primary tumor tissues and cancer cell lines by direct sequence analysis or MSP. QMSP was developed for *GULP1* gene for high throughput analysis in multiple set of primary ovarian tissues including normal ovarian epithelium, benign growth and primary tumor tissues. Functional characterization of GULP1 was also performed.

**Figure 2. *GULP1* methylation inversely correlated with mRNA and protein expression level. A.** DNA isolated from ovarian cancer and normal cell-lines was subject to bisulfite treatment; and methylation status of the CpG island within the *GULP1* was assessed by bisulfite sequencing analysis (left panel) or MSP (right panel). Pink boxes indicate the location of CpG sites. Unmethylated cytosines are converted to uracil and detected as adenine while methylated cytosine detected as guanine. U - unmethylated DNA, M - methylated DNA. **B.** *GULP1*

methylation in 15 primary OC (top) and 13 normal ovarian epithelial tissue (bottom) determined by conventional methylation specific PCR (MSP). U - unmethylated DNA, M - methylated DNA. **C.** The expression levels of the *GULP1* mRNA in 15 primary OC tissues (red) and 10 normal ovarian surface epithelial washing samples (blue) determined by Affymetrix U133 Plus 2.0 expression array analysis. **D.** RT-PCR (top panel) and western blot (WB) (lower panel) showing the expression status of GULP1 at the RNA and protein levels in the indicated cell lines. *GAPDH* and β-actin was used as loading controls for RT-PCR and WB respectively. **E.** mRNA expression of *GULP1* determined by RNA-seq analysis in the TCGA OC cohort [OC, n=569 (red), normal ovarian epithelium, n=8 (blue); p =0.0001]. **F.** *GULP1* mRNA expression in the TCGA cohort was categorized as high level (one standard deviation above the mean) or low level (one standard deviation below the mean), and (**G**) *GULP1* methylation was assessed in TCGA tumors with high *GULP1* expression (blue, n=83) and tumors expressing low levels of *GULP1* (red, n=16). p=0.0001.

**Figure 3. *GULP1* methylation is associated with advanced disease and worse survival of ovarian cancer patients. A.** *GULP1* methylation was assessed by QMSP in a training set containing 61 epithelial ovarian cancers and 13 normal ovarian epithelium. By using an optimal cutoff of 0.72, 34% (21/61) of the tumor samples were found to be hypermethylated in comparison to 0% (0/13) of the normal ovarian epithelium samples (p=0.03). The scatter plot shows the samples categorized as unmethylated or methylated based on detection of methylation above the cut-off (Y-axis, quantity of methylated allele (GULP1/β-actin × 1000). **B.** *GULP1* methylation was assessed by QMSP in 365 epithelial ovarian cancers, 16 borderline ovarian tumors, 18 cystadenomas and 13 normal ovarian epithelial tissues. The scatter plot shows the

samples categorized as unmethylated or methylated based on detection of methylation values above the same cut-off as noted above (Y-axis, quantity methylated allele (log 10 of GULP1/β-actin × 1000). **C.** 365 ovarian tumors (independent cohort) were classified as early (stage I and II) or advanced (stage III and IV) disease. Scatter plots showing quantitative *GULP1* methylation values in early (triangles) and advanced (circles) stage ovarian tumors ($p<0.001$). **D.** 365 ovarian tumors (independent cohort) were classified as low or high grades. Scatter plots of *GULP1* methylation values of low (triangles) and high (circles) grade ovarian tumors ($p<0.033$). **E.** Stratification of independent set by presence or absence of residual disease (smaller or larger and equal 2cm). Scatter plots of *GULP1* methylation values in <2cm (triangles) and ≥2cm (circles) residual disease ($p<0.0008$). **F.** Kaplan Meier estimates of overall survival based on *GULP1* methylation status in the independent cohort (n=365) of ovarian cancer patients (unmethylated - blue line, methylated - green line) ($p=0.02$). **E.** Kaplan–Meier estimates of disease specific survival based on the *GULP1* methylation status in the independent cohort (n=365) of ovarian cancer patients (unmethylated - blue line, methylated - green line) ($p=0.011$).

**Figure 4.** ***GULP1 modulates ovarian cancer cell viability and colony formation.***

**A.** Forced expression of GULP1 in IGROV cells using lentivirus-encoded GULP1-GFP. Cell lysates were collected from GULP1-expressing (GULP1-GFP) cells and control cells infected with empty vector (E.V.) and analyzed by western blot for the expression of indicated proteins. β-actin was used a loading control. **B.** IGROV-GULP1-GFP and control IGROV-E.V. cells were plated at equal numbers in triplicates and relative cell viability was determined using an Alamar Blue assay at indicated times points. **C.** GULP1 expression was knocked down in A2780 cells by stable expression of short-hairpin RNA. Cell transfected with empty or scramble vectors

were used as controls. Whole cell lysates were prepared from *GULP1*-depleted (A2780-shGULP1) and control (A2780-E.V. and A2780-scramble) cells and analyzed by western blot for the GULP1 expression. β-actin was used as a loading control. **D.** *GULP1* depleted and control IGROV cells were plated at equal numbers in triplicates and relative cell viability was determined using an Alamar Blue assay at indicated times points. **E.** Colony formation assay: GULP1-overexpressing (2008-GULP1-GFP) or control (2008-E.V.) cells were treated with G418 for 14 days. Colonies were stained, scanned and quantified with GelCount Colony Counter. **F.** Matrigel Boyden chamber invasion assay: 2008-GULP1-GFP and 2008-E.V. cells were allowed to invade through the Matrigel for 36h and invaded cells were stained with H&E. Images were captured under a light microscope at x200 and stained cells were automatically quantified with ImageJ. **G.** 2008-GULP1-GFP and control 2008-E.V. cells were plated at equal numbers in triplicates and relative cell viability was determined using an Alamar Blue assay at indicated times points.

**Figure 5.** ***GULP1 expression correlates with dysregulation of cancer promoting pathways.***

**A.** *GULP1* RNA-Seq mRNA expression in the TCGA ovarian cancer cohort (n=569) was categorized as high level (one standard deviation above the mean) or low level (one standard deviation below the mean) and pathway activation strength (PAS) values have been calculated according to iPANDA algorithm. Hierarchically clustered heatmap represents differentially activated pathways in 16 tumors with low *GULP1* mRNA expression (83 tumors with high *GULP1* expression were used as a reference). Downregulated PAS values for each sample/pathway are indicated in blue, whilst upregulated PAS values are shaded in red. **B.** Cell lysates were collected from GULP1-expressing (GULP1-GFP) cells and control cells infected

with empty vector (E.V.) and analyzed by western blot for the expression of indicated proteins. β-actin was used as a loading control. **C.** Whole cell lysates were prepared from *GULP1*-depleted (A2780-shGULP1) and control (A2780-E.V. and A2780-scramble) cells and analyzed by western blot for the expression of indicated proteins. β-actin was used as a loading control.

**Table 1.** Demographic and clinical characteristics of ovarian cancer patients

**A.** Training set and Normal controls; **B.** Independent validation set with Borderline Tumors and Cystadenoma; **C.** Association between GULP1 methylation and clinicopathological factors by logistic regression.

**Table 1. Demographic and clinical characteristics of ovarian cancer patients**

**A**. Training set and Normal controls; **B**. Independent validation set with Borderline Tumors and Cystadenoma; **C.** Association between GULP1 methylation and clinicopathological factors by logistic regression.

**A. Training Set**

| | **Training set (n=61)** | **Controls (n=13)** |
|---|---|---|
| **Age at diagnosis** | | |
| Median | 57 | 46 |
| Range | 37-81 | 40-55 |
| **Race** | | |
| Caucasian | 58 | 0 |
| African-american | 0 | 0 |
| Hispanic | 0 | 13 |
| Unknown | 3 | 0 |
| **Histology** | | |
| Serous-papillary | 41 | |
| Endometrioid | 6 | |
| Mucinous | 2 | |
| Undifferentiated | 1 | |
| Unknown | 11 | |
| **Stage** | | |
| I | 13 | |
| II | 9 | |
| III | 38 | |
| IV | 0 | |
| Unknown | 2 | |
| **Grade** | | |
| G1 | 11 | |
| G2 | 9 | |
| G3 | 30 | |
| Unknown | 11 | |

**B. Validation set**

| **Ovarian cancer patients n=365** | |
|---|---|
| **Age at diagnosis** | |
| Median | 61 |
| Range | 21-89 |
| **Follow-up time (months)** | |
| Range | 0-234 |
| Unknown n=1 | |
| **Histology** | n |
| Serous | 222 |
| Mucinous | 43 |
| Endometrioid | 38 |

| | |
|---|---|
| Clear cell | 17 |
| Adenocarcinoma | 13 |
| Unknown | 32 |
| | |
| **Grade** | |
| Low (I/II) | 157 |
| High (III/IV) | 202 |
| Unknown | 6 |
| | |
| **Stage** | |
| Early (I/II) | 95 |
| Advanced (III/IV) | 270 |
| | |
| **Residual disease after surgery** | |
| <2 cm | 180 |
| >2 cm | 157 |
| Unknown | 28 |

| | |
|---|---|
| **Borderline tumors n=16** | |
| | |
| **Age at diagnosis** | |
| Median | 50.5 |
| Range | 19-77 |
| *Unknown (n=4)* | |

| | |
|---|---|
| **Cystadenoma n=18** | |
| | |
| **Age at diagnosis** | |
| Median | 30 |
| Range | 26-55 |
| *Unknown (n=15)* | |

**C. Association between GULP1 methylation and clinicopathological factors by logistic regression.**

| | *OR | 95% ¶C.I. | | P-value |
|---|---|---|---|---|
| Age (continuous) | **1.03** | **1.01** | **1.05** | **0.000** |
| Age (=>61) | **1.82** | **1.19** | **2.77** | **0.006** |
| Histology (serous) | **1.69** | **1.04** | **2.72** | **0.033** |
| Grade (III/undifferentiated) | **1.6** | **1.04** | **2.45** | **0.033** |
| Stage (III/IV) | **2.34** | **1.4** | **3.92** | **0.001** |
| Residual disease after surgery (= | **2.24** | **1.44** | **3.49** | **0.000** |

*OR=Odd Ratio; ¶C.I= Confidence Interval

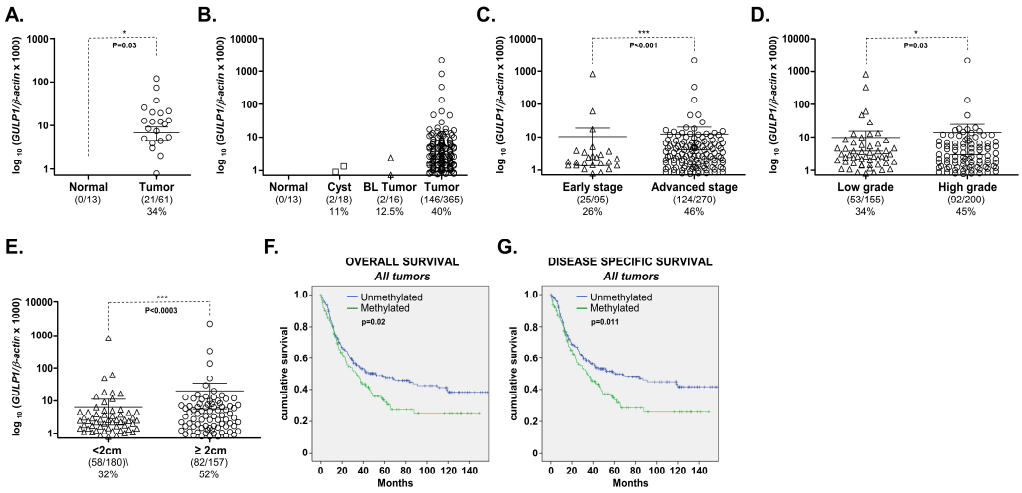


**Figure 3**

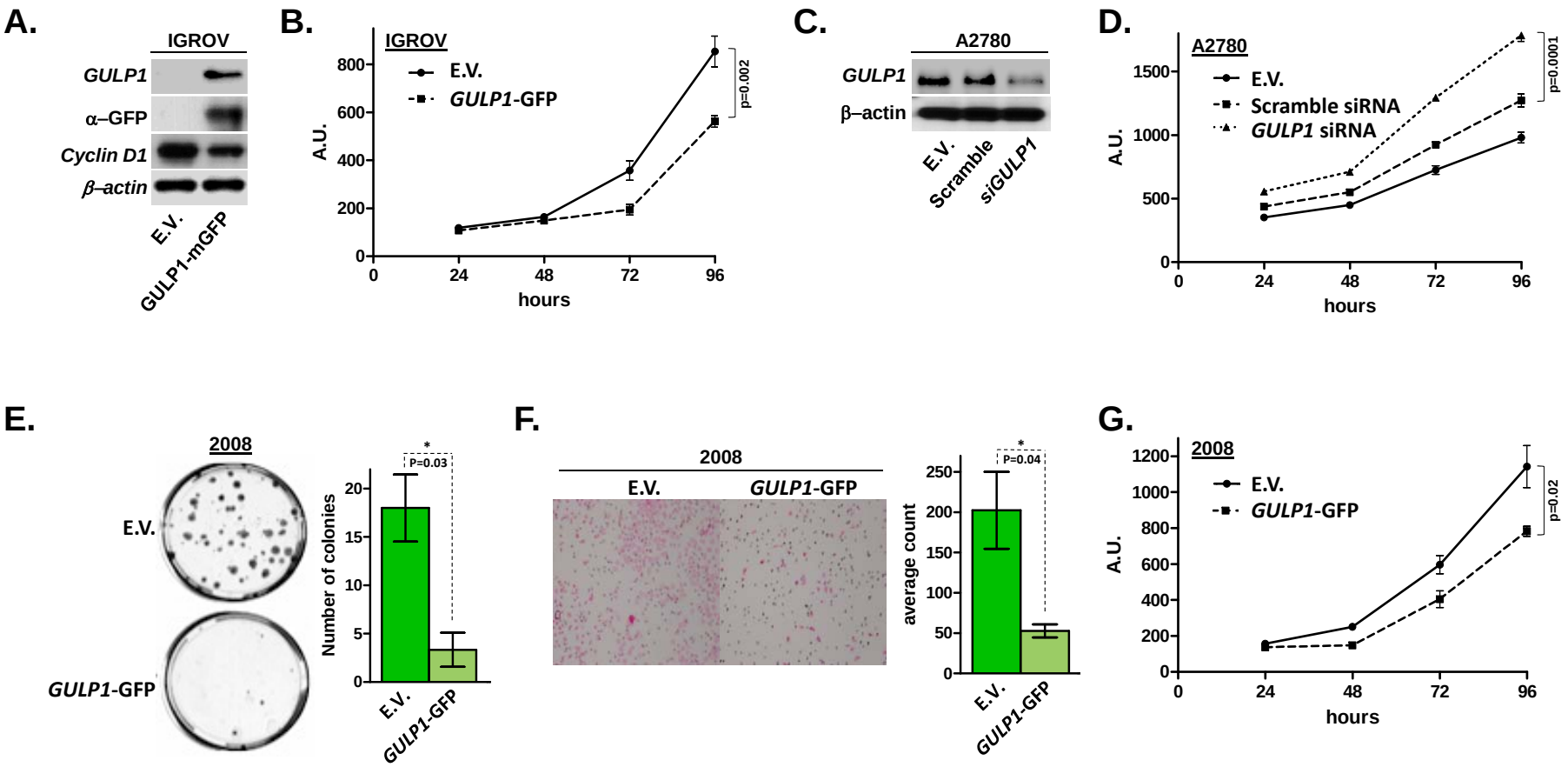
A.
IGROV
GULP1
α–GFP
Cyclin D1
β–actin
E.V.
GULP1-mGFP
B.
IGROV
E.V.
GULP1-GFP
A.U.
hours
p=0.002
C.
A2780
GULP1
β–actin
E.V.
Scramble
siGULP1
D.
A2780
E.V.
Scramble siRNA
GULP1 siRNA
A.U.
hours
p=0.0001
E.
2008
E.V.
GULP1-GFP
Number of colonies
P=0.03
F.
2008
E.V.
GULP1-GFP
average count
P=0.04
G.
2008
E.V.
GULP1-GFP
A.U.
hours
p=0.02

**Figure 4**

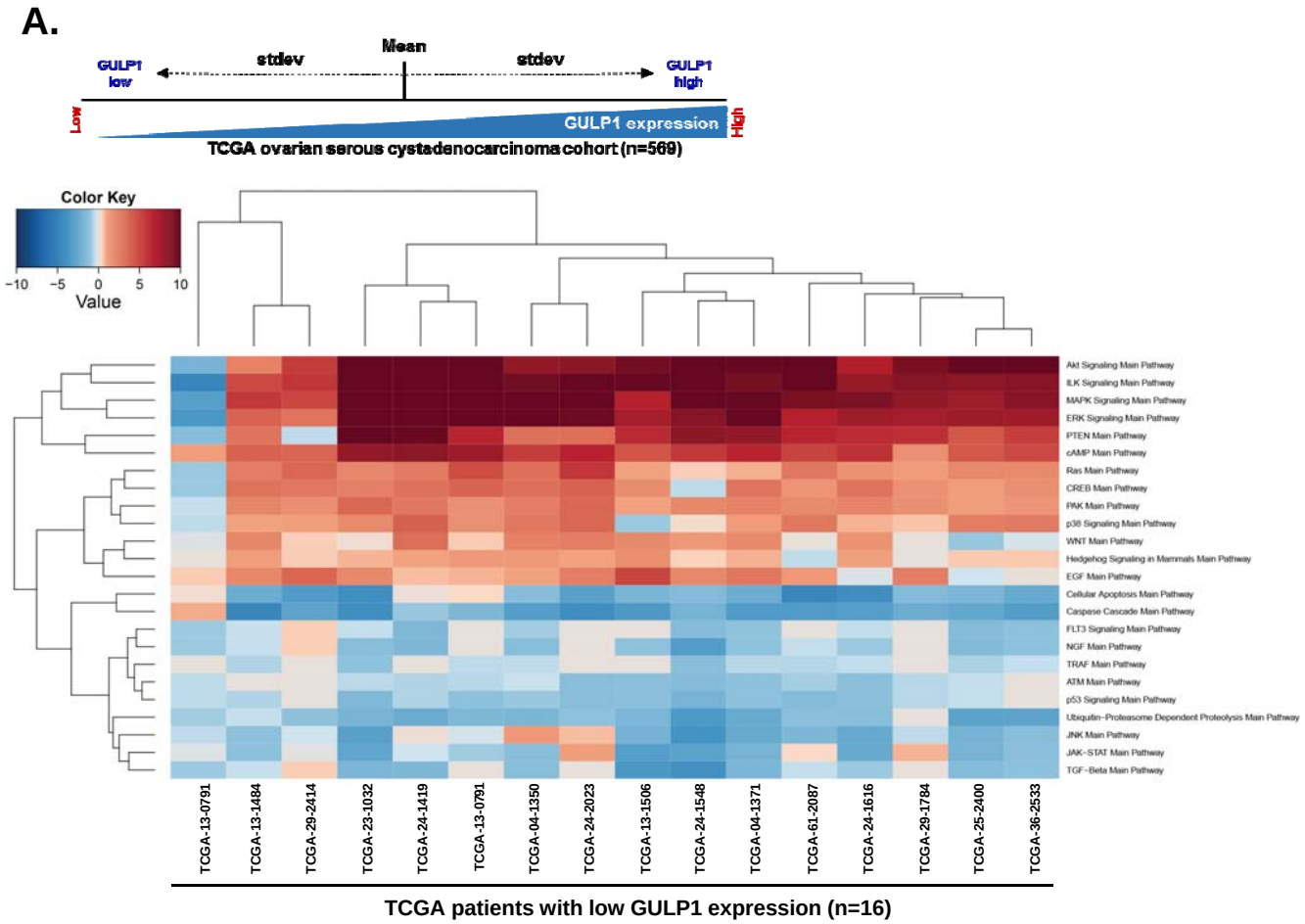
A.
GULP1 low
stdev
Mean
stdev
GULP1 high
Low
GULP1 expression
High
TCGA ovarian serous cystadenocarcinoma cohort (n=569)
Color Key
−10 −5 0 5 10
Value
Akt Signaling Main Pathway
ILK Signaling Main Pathway
MAPK Signaling Main Pathway
ERK Signaling Main Pathway
PTEN Main Pathway
cAMP Main Pathway
Ras Main Pathway
CREB Main Pathway
PAK Main Pathway
p38 Signaling Main Pathway
WNT Main Pathway
Hedgehog Signaling in Mammals Main Pathway
EGF Main Pathway
Cellular Apoptosis Main Pathway
Caspase Cascade Main Pathway
FLT3 Signaling Main Pathway
NGF Main Pathway
TRAF Main Pathway
ATM Main Pathway
p53 Signaling Main Pathway
Ubiquitin−Proteasome Dependent Proteolysis Main Pathway
JNK Main Pathway
JAK−STAT Main Pathway
TGF−Beta Main Pathway
TCGA-13-0791
TCGA-13-1484
TCGA-29-2414
TCGA-23-1032
TCGA-24-1419
TCGA-13-0791
TCGA-04-1350
TCGA-24-2023
TCGA-13-1506
TCGA-24-1548
TCGA-04-1371
TCGA-61-2087
TCGA-24-1616
TCGA-29-1784
TCGA-25-2400
TCGA-36-2533
TCGA patients with low GULP1 expression (n=16)

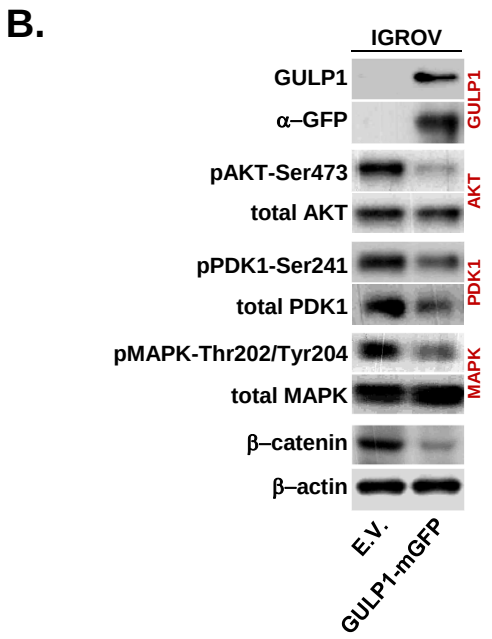
B.
IGROV
GULP1
α–GFP
GULP1
pAKT-Ser473
total AKT
AKT
pPDK1-Ser241
total PDK1
PDK1
pMAPK-Thr202/Tyr204
total MAPK
MAPK
β–catenin
β–actin
E.V.
GULP1-mGFP

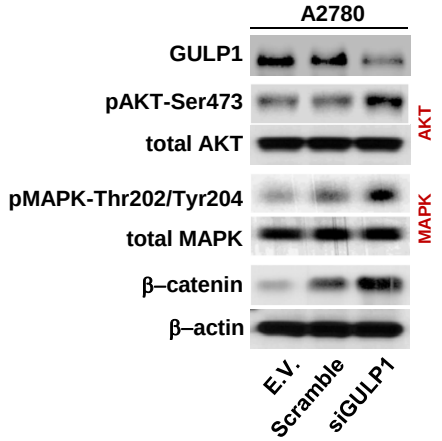
C.
A2780
GULP1
pAKT-Ser473
total AKT
AKT
pMAPK-Thr202/Tyr204
total MAPK
MAPK
β–catenin
β–actin
E.V.
Scramble
siGULP1

**Figure 5**

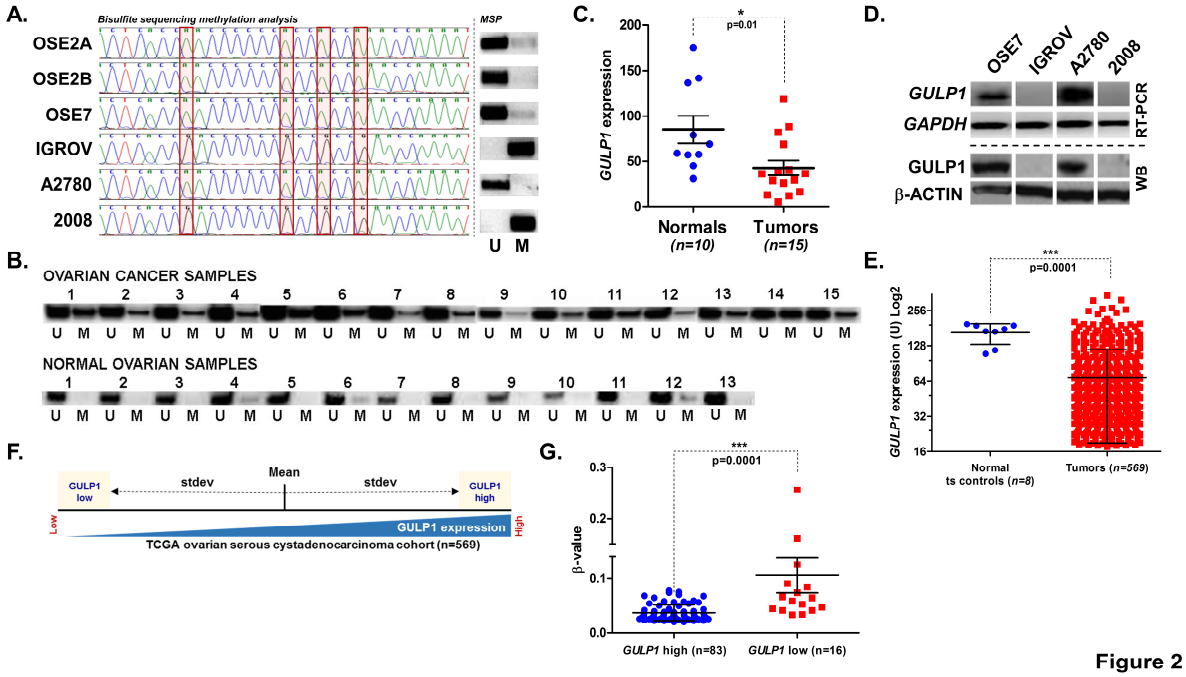


**Figure 2**

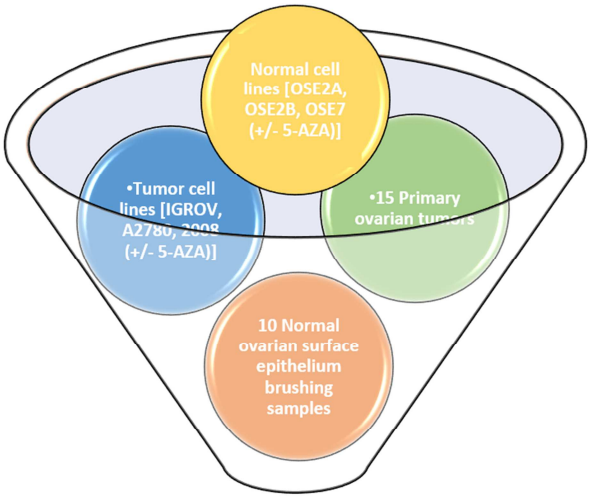


**•Affymetrix U133 Plus 2.0 array (*>54,000 probes*)**

- Genes differentially expressed between normal samples/cell-lines and tumor samples/cell-lines
- Genes that have a low expression level in cancer samples and cell lines
- Genes differentially expressed between 5-AZA or mock-treated cancer cell-lines (re-activation)

**88 genes**

Excluded

- **22 genes -suitable primers could not be designed**
- **12 genes without promoter CpG island**
- **9 genes -probes located outside of the promoter**
- **2 genes already studied in ovarian cancer**

**43 genes**

**Validation by bisulfite sequencing**
*(GULP1, CLIP4, BAMBI, NT5E, TGFB2)*

***GULP1***

**Integrated Transcriptomic and Epigenomic Analysis of Ovarian Cancer Reveals Epigenetically Silenced *GULP1***

Highlights

- *GULP1* is specifically methylated in ovarian cancer
- *GULP1* is associated with clinicopathological parameters in ovarian cancer patients
- *GULP1* is a potential tumor suppressor gene